

NUMERICAL SIMULATION OF GAS DYNAMIC FLOW IN RESONATING SYSTEMS

Anton V. Primakov¹, Alexander A. Zhilin^{1,2}

¹Khristianovich Institute of Theoretical and Applied Mechanics SB RAS,
Novosibirsk, Russia

²Siberian State University of Water Transport, Novosibirsk, Russia

Abstract. Gas-dynamic flows in channel systems with active generation of high-intensity oscillations are investigated using numerical simulation in ANSYS Fluent. Flow patterns in channels determine the gas-dynamic parameters of the system and establish cellular structure formation features near resonator are obtained. The distance between the nozzle section and the resonator edge influence on the gas-dynamic characteristics of acoustic-convective flow in the two-channel system path is revealed. Three characteristic nozzle-resonator distances are considered. In the case of the smallest gap, high-frequency oscillations are recorded. In this case, the value of average pressure in resonator path is the maximum of the considered cases. With an increase in gap between the resonator edge and the nozzle section, generated vibrations from high-frequency oscillations with low amplitude are converted to a pure tone with high amplitude. At the maximum distance, there is a transition of fundamental oscillation frequency to a half harmonic with a redistribution of oscillation energy into multiple harmonics.

Keywords: Hartmann's whistle, resonant systems, high-intensity acoustic sensations, wave sensations, off-design jet

Acknowledgments: the work was carried out on the topic of the state assignment (state registration No. 121030500163-4) and was partially supported by the Russian Foundation for Basic Research (grant No. 20-31-90117).

For citation: Primakov A.V., Zhilin A.A. Numerical simulation of gas dynamic flow in resonating systems. *News of Higher Educational Institutions. Construction.* 2022; (3): 112–119. (In Russ.). DOI: 10.32683/0536-1052-2022-759-3-112-119.

Introduction. Air flows are actively used in various areas of human activity. Everyday life is not complete without devices, the principle of operation of which is based on air flows use. Such devices include ventilation and heat removal devices [1]. Air flows are an environment in which acoustic vibrations can freely propagate, which is widely used in the device of gas-dynamic sirens and whistles [2, 3], some of them are used to dehumidify various materials. Air flowing around materials helps to extract moisture from it [4, 5], and the impact on the material by acoustics allows to intensify the process without damaging substance structure [6], which is useful in chemical [7], food [8–11] and construction industry [12–15]. Some gas-dynamic oscillation generators have great potential in the field of drying materials. Such a device is a Hartmann-type generator or Hartmann whistle. The design of Hartmann generator includes a jet flow source and a resonator tank into

which the jet flows. As it fills, pressure increases in the resonant cavity, which leads to its emptying and interaction with the jet. As a result of the interaction, a high-intensity oscillation is generated, propagating in the near field of the generator. The phenomena and wave processes created by this device have become the subject of many studies [16]. Various configurations of Hartmann generators are of particular interest, both in industry and in science, since the gas-dynamic flows flowing in cavities have not been fully studied. One of the most important parameters of the Hartmann oscillator system is the distance between the nozzle and the resonator. Many works have been devoted to this parameter study, but no consensus has been reached on the optimal geometry, since each system configuration has unique flow features [17]. The study [18] conducted experimentally revealed Hartmann effect existence areas. When the resonator is placed in such an area, high-intensity vibrations occur, i.e. resonance occurs. At the same time, there may be several such areas due to the periodic structure of the jet. This work is the ideological legacy of a number of studies, the first of which is described above. Further work is aimed at creating a numerical copy of the channel system generating a gas-dynamic flow with powerful acoustic vibrations [19–23].

Physical and mathematical description of the problem. In numerical modeling, the geometry under study is represented by two perpendicular intersecting channels (Fig. 1). The first channel is the Hartmann whistle consisting of a subsonic tapering nozzle with a diameter of $0,5d$ (I) and a coaxially arranged cylindrical resonator d (II). The second channel of the square section works as a secondary resonator with a closed end wall (III), and a working part with a free outlet (IV).

The computational domain constructed for numerical simulation is a derivative of a multi-block structured grid system of hexahedral and polyhedral elements thickening to the walls. The study was carried out in an axisymmetric formulation. At the initial moment, an overpressure $P = 6$ atm, is set at the entrance to the pre-chamber, and a value corresponding to normal conditions is set in the rest of the calculation area. The gas flow inside the system under consideration is investigated. A gas adhesion condition is set on the surface of a rigid wall. The position of the resonant cavity varies relative to the nozzle edge. Three characteristic distances are selected: $S_1 = 0,85d$, $S_2 = 1,35d$, $S_3 = 1,85d$, and the flow parameters are determined at points near the end of the cavity and in the system center of the: monitor 1 and 2.

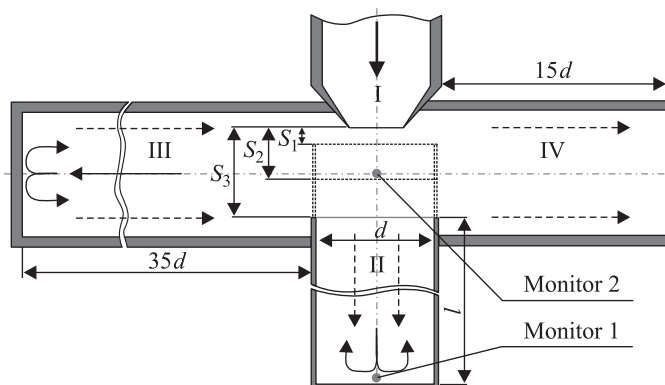


Fig. 1. Schematic representation of a channel-free system

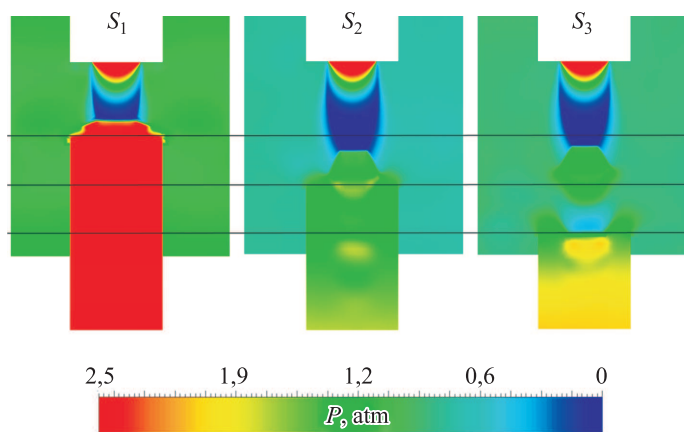


Fig. 2. Flow patterns in the central region of the system

Numerical simulation was carried out in the ANSYS Fluent software package. A three-dimensional nonstationary problem is solved using the Navier–Stokes equations averaged over Favre and supplemented with a k – ω turbulence model [24].

Flow pattern. Let's consider the steady-state process and the moment of filling the resonant cavity with a jet is chosen as a reference point. The propagation process and waves interaction in the cavity is described in detail in [25]. Consider the flow patterns in the central part and resonator of the channel system (Fig. 2) during the wave's advance to the closed end. It is easy to distinguish differences in flow parameters for channel configurations with different distances between the nozzle and the resonant cavity.

In the case with the smallest gap of $0,85d$ the absorption process and resonator emptying weakly resembles the Hartmann effect. The resonator is filling with small volumes of gas. Wave interactions are constantly occurring inside the cavity, due to which a quasi-constant increased pressure of an average of 2,5 atm is maintained in the resonator. The jet is constantly in a deformed state, in addition, the resonator is located in an area where the pressure decreases with the flow acceleration. The pressure in this place is close to 0 atm. Placing the resonator in this area leads to a sharp increase in pressure up to 2,5 atm in front of the edge. Comparison of the diameters of the $0,7d$ jet and the $1d$ resonator shows that it is impossible to overlap the cavity with such a flow. As a result, there is a constant loss of gas near the resonator walls.

Increasing the nozzle-resonator distance to $1,35d$ leads to the Hartmann effect, since the resonator is placed in the jet optimal area [19] with high pressure. The pressure in front of the edge of the cavity does not allow the returning flow to flow out, which leads to rapid filling of the cavity. The compression wave created by the jet reaches the end of the cavity and returns to the resonator open edge, leaving a high pressure of up to 4,7 atm behind the wave front. When the resonant cavity is emptied, a counter-directional flow occurs to the jet. In other words, the Hartmann effect is observed. In this case, pressure fluctuations in the resonator occur with a large amplitude up to 3,3 atm. The jet covers the cavity by 95 %, which does not allow significant pressure losses to occur when flows flow through the walls.

In the latter case, the resonator is located in the jet second barrel area at a distance of $1,85d$ from the nozzle. In this case, the jet does not have enough energy (as a result of dissipation at the boundaries) to lock the resonator. There is a constant outflow of response flows along the cavity walls, which prevents filling. By the time the compression wave reaches the resonator edge, the pressure will not be high enough $\sim 3,8$ atm. The transition to the resonator emptying stage will be recorded only after the second wave reaches the resonator edge, and a pressure of up to $3,5$ atm is established in the cavity in the end face area. At the same time, the pressure at the resonator edge does not exceed $2,9$ atm, as a result, a pressure gradient is formed in the resonator. The ratio of the jet diameter to the cavity diameter is $0,36$. However, there is no sharp increase in pressure in front of the cavity and locking does not occur. Air is constantly leaking significantly from the resonator, including at the filling stage. In this case, two areas of pressure build-up near the edge inside the resonator are most clearly distinguished.

Pressure distributions in the black-and-white spectrum are shown in Fig. 3 (*a-c* is the resonant cavity filling stage, and *d-f* is the resonator emptying stage). Note that in the case of S_1 the expiration occurs even when the cavity is filled (Fig. 3, *a*). Fig. 3, *d* shows that the response flows intensify at the outflow phase, forming vortices in the working part. At the same time, there is a noticeably increased pressure in the working part walls area, relative to other configurations. In the case of S_2 at the filling stage, the jet completely locks the resonator (Fig. 3, *b*), and the emptying is accompanied by response flows less significant than in the case of S_1 (Fig. 3, *e*). At the maximum gap S_3 the formed first barrel of the jet is clearly visible, and in the area of the second barrel there is a sealing area at the resonator filling stage (Fig. 3, *c*). The stage of emptying the resonator is associated with the occurrence of powerful flows resulting from a collision with a jet (Fig. 3, *f*).

Gas dynamic flow parameters. In order to track changes in gas dynamic parameters over time, spot monitors were installed at characteristic points of

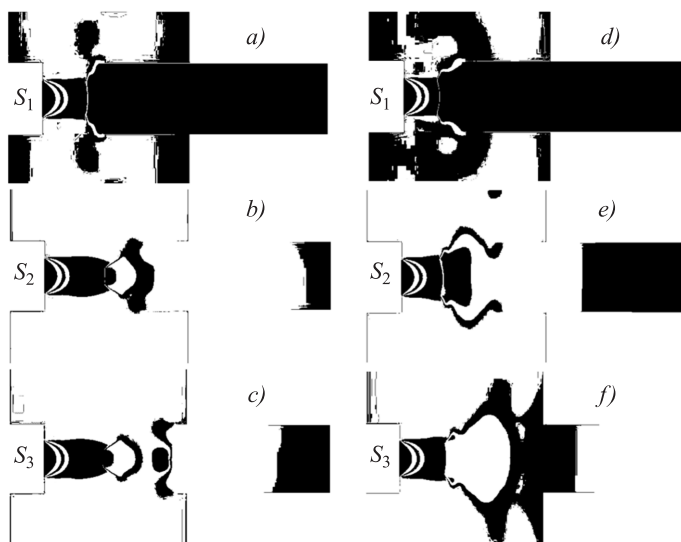


Fig. 3. Flow patterns in the central region of the system in the black-and-white spectrum

the channel system. Of greatest interest are the areas near the resonant cavity, where the greatest vibrations values are achieved, in the center of the system, where the jet is formed and the response flow collides with the jet, and in the working part of the system, since data verification with experiment is possible at this point. The figures show comparisons of pressure waveforms for configurations with different distances between the nozzle and the resonator at the points of the system described above. The time range of 4 ms is considered for the case with the smallest gap, in view of the high-frequency nature of the signal, (S_1) and 20 ms for other configurations. In these graphs, special attention should be paid to the amplitude and oscillations shape. Pressure distributions are presented in the form of amplitude-frequency spectra in the figures for analyzing changes in the tonal structure of signals in different configurations. With a minimum gap (S_1 in Fig. 4) the amplitude is unstable and ranges from 0,05 to 0,09 atm. The oscillations have a sinusoidal shape with a clear extremum and a period $T = 0,2$ ms. The frequency of this oscillation was 4,8 kHz, and the intensity of the dominant harmonic was 150 dB. Multiple harmonics are easily detected, but their intensity is comparable to the noise level.

When the nozzle-resonator gap increases to (S_2 in Fig. 4) the oscillations acquire a trapezoidal shape, with a constant output at the maximum value. The amplitude of the oscillations remains unchanged and is 3,35 atm and the average value is 2,64 atm. The oscillation period is $T = 3,6$ ms, while $T = 1,7$ ms retains the highest pressure value. A pure tone with a fundamental frequency of 274 Hz and an intensity of 183 dB is observed in the oscillation spectrum. The second harmonic at 558 Hz has an intensity of 172 dB, and the third at 832 Hz has 169 dB.

The case with the largest gap (S_3 in Fig. 4) differs in the shape of the oscillation. The output to the maximum value occurs twice, which is justified by insufficient jet pressure. As a result, the oscillation period increases to $T = 7$ ms, there is no constant output, but there is a slight increase in pressure from 3,2 to 3,6 atm during 1,7 ms. At the same time, the average pressure value is 2,73 atm, and the oscillation amplitude is 2,86 atm. The dominant frequency in the spectrum for this configuration is at 288 Hz and has an amplitude of 184 dB, but it is not the main one. The first harmonic in this frequency response is tone at 144 Hz with

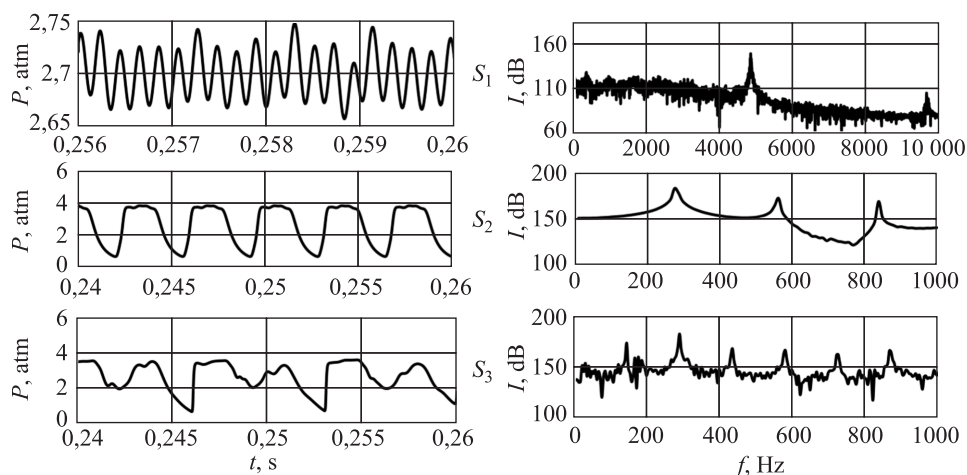


Fig. 4. Pressure distribution and frequency response near the end face

an intensity of 174 dB. In other words, in this configuration there was a transition of the fundamental frequency to the half harmonic. There are also twice as many harmonics in the spectrum, which confirms the face of such a transition. The amplitude of multiple harmonics is relatively constant 163–169 dB.

Consider the data from monitor 2 in the area where the jet is formed. With a small nozzle-resonator distance (S_1 in Fig. 5) the oscillations realigned, and the oscillations amplitude for all periods ($T = 0,3$ ms) is 0,18 atm. The shape of the oscillation changes: after the transition of the extremum point, there is an output to a constant value, which lasts 0,03 ms. The fundamental frequency at this point was 4,8 kHz, and the intensity of the fundamental harmonic was 157 dB. The increase in the oscillations amplitude is caused by the constant collision of the jet with the response flow.

In the case of (S_2 in Fig. 5) the distribution area with the maximum value changes: there are several maxima and areas with a constant value, also at the end of each oscillation there is a sharp increase in pressure, followed by a sharp drop and an exit to the “shelf” within 0,21 ms. The oscillation period is $T = 2,2$ ms, and a constant minimum (0,27 atm) is observed between the oscillations for 1,25 ms. The oscillation amplitude is 2,32 atm. In the amplitude-frequency spectrum, the occurrence of signal noise is visible. The main frequency is 274 Hz with an intensity of 181 dB. The second harmonic is 165 dB, and the third is 170 dB.

In the case of the largest distance between the nozzle and the resonator (S_3 in Fig. 5) fluctuations are distinguished in the pressure distribution over time, reaching a constant value. However, every second oscillation differs from the previous one by a different number of maxima. Between the oscillations, a constant minimum pressure value (0,11 atm) was recorded for 2,2 ms. The oscillation period is from 1,2 to 1,8 ms. The oscillation amplitude is 1,3–1,5 atm. The frequency of the main oscillation is 143 Hz, and its intensity is 168 dB. The dominant second harmonic has an intensity of 177 dB. The intensity of multiple harmonics varies from 156–173 dB.

Conclusion: the influence of the distance between the nozzle and the resonant cavity on the process of oscillation formation in the two-channel system is investigated. In the case of a close location of the nozzle and the resonator, the cavity is frequently filled with small volumes of air. As a result, vibrations with

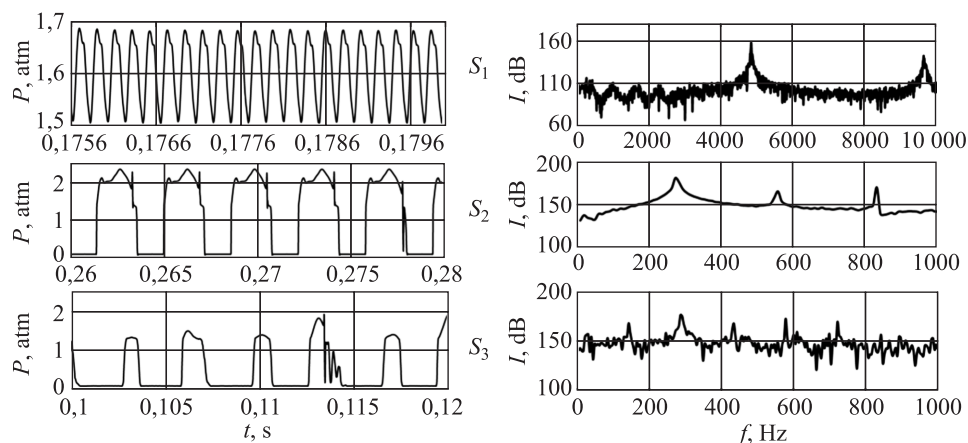


Fig. 5. Pressure distribution and frequency response in the center of the system

a low intensity of 131 dB and a frequency of 4,8 kHz are generated, while a pressure of about 2,5 atm is set inside the resonator. As the distance to S_2 increases, a pure tone is observed and the optimal mode with an intensity of 166 dB at 274 Hz is realized, i.e. the classical flow in the Hartmann generator is realized. With a large gap, the intensity of the generated oscillations decreases to 163 dB at 288 Hz and the appearance of subharmonics.

References

1. Baev V.K., Fedorov A.V., Fomin V.M., Khmel' T.A. Centrifugal convection in rapid rotation of bodies made of cellular-porous materials. *Prikladnaya mekhanika i tekhnicheskaya fizika = J. of applied mechanics and technical physics*. 2006; 47(1): 36–46. (In Russ.).
2. Vyal'tsev V.V., Khorguani V.G. Powerful low-frequency sound siren. *Akusticheskiy zhurnal = Acoustic magazine*. 1961; 7(3): 377–378. (In Russ.).
3. Chanaud R.C. Experiments concerning the vortex whistle. *J. of the Acoustical Society of America*. 1963; 35(7): 953–960.
4. Zhilin A.A., Fedorov A.V., Grebenshchikov D.M. Dynamics of acousto-convective drying of sunflower cake compared with drying by a traditional thermo-convective method. *Foods and Raw Materials*. 2018; 6(2): 370–378.
5. Fedorov A.V., Zhilin A.A., Korobeinikov Yu.G. Investigation of the processes of impregnation and drying of granular silica gel. *J. Eng. Phys. Thermophys.* 2011; 84(5): 965–974.
6. Zhilin A.A., Fedorov A.V. Acoustoconvective drying of pine nuts. *J. Eng. Phys. Thermophys.* 2014; 87(4): 908–916.
7. Zhilin A.A., Fedorov A.V. Acoustoconvection drying of meat. *J. Eng. Phys. Thermophys.* 2016; 89(2): 923–933.
8. Zhilin A.A., Fedorov A.V. Acoustoconvective drying of cellular gas concrete. *J. Eng. Phys. Thermophys.* 2017; 90(6): 1412–1426.
9. Hartmann J., Troll B. On a new method for the generation of sound waves. *Phys. Rev.* 1922; 20(11): 719–727.
10. Hartmann J., Trolle B. New investigation of the air-jet generator for acoustic waves. *Dann. Mat. Fys. Medd.* 1930; 7(6): 1–38.
11. Hartmann J. On the production of acoustic waves by means of an air-jet of a velocity exceeding that of sound. *Phil. Magazine*. 1931; 11: 926–948.
12. Raman G., Shrinivasan K. The powered resonance tube: from Hartmann's discovery to current active flow control applications. *Progress in Aerospace Science*. 2009; 45: 97–123.
13. Kurkin V.P. Sound generated by a gas-jet siren. *Acoustic magazine*. 1961; 7(4): 442–445.
14. Brun E., Boucher R.M.G. Research on the acoustic air-jet generator: a new development. *J. of the Acoustical Society of America*. 1957; 29(5): 573–583.
15. Brocher E., Maresca C., Bournay M.H. Fluid dynamics of the resonance tube. *J. of Fluid. Mech.* 1970; 43(2): 369–384.
16. Murugappan S., Gutmark E. Parametric study of the Hartmann-Sprenger tube. *Experiments in Fluids*. 2005; 38(6): 813–823.
17. Narayanan S., Bholanath Behera, Sundararajan T., Srinivasan K. Acoustic heating effects in Hartmann whistle. *International Journal of aeroacoustics volume*. 2013; 12(5& 6): 557–578.
18. Rozenberg L.D. Sources of powerful ultrasound. Moscow: Nauka, 1967. P. 7–110. (In Russ.).

19. Glaznev V.N., Korobeinikov Yu.G. Hartmann effect. Region of existence and oscillation frequencies. *J. of Appl. Mech. Tech. Phys.* 2001; 42(4): 616–620.
20. Fedorov A.V., Fedorchenko I.A., An S.B. et al. Physical and mathematical modeling of acoustoconvective drying of rice. *Inzhenerno-fizicheskiy zhurnal = Journal of Engineering Physics and Thermophysics.* 2010; 83(1): 64–73. (In Russ.).
21. Fedorchenko I.A., Fedorov A.V. Mathematical simulation of acoustic and gas-dynamical processes in the channel of an acoustoconvective dryer. *Inzhenerno-fizicheskiy zhurnal = Journal of Engineering Physics and Thermophysics.* 2013; 86(4): 685–688. (In Russ.).
22. Primakov A.V., Zhilin A.A. Studying of the resonator depth influence on amplitude-frequency characteristics operating flow in the two-channel system. *Journal of Physics: Conference Series.* 2019; 1404: 012096.
23. Primakov A.V., Zhilin A.A. Gas-dynamic studying of the two-channel system flow using numerical simulation methods. *AIP Conference Proceedings.* 2020; 2288: 030060.
24. Menter F.R. Two-equation eddy-viscosity turbulence models for engineering applications. *AIAA Journal.* 1994; 32(8): 1598–1605.
25. Zhilin A.A., Primakov A.V. Numerical study of thermal effects in an acoustic-convective flow in a bichannel system. *Teplofizika i aeromekhanika = Thermophysics and Aeromechanics.* 2022; 29(1): 79–89. (In Russ.).

Information about the authors

A.V. Primakov – Post-graduate Student, Research Engineer, primakow@itam.nsc.ru

A.A. Zhilin – PhD, Ass. Professor, lab20@itam.nsc.ru

Contribution of the authors: the authors contributed equally to this article. The authors declare no conflicts of interests.

The article was submitted 21.01.2022

Approved after reviewing 21.02.2022

Accepted for publication 28.02.2022